Climate Dynamics manuscript No.
(will be inserted by the editor)

Relationship between sudden stratospheric warming and tropospheric blocking as simulated by the multi-century IPSL-CM5A coupled climate model

Jessica Vial · Tim J. Osborn

Received: date / Accepted: date

Abstract It is widely believed that there is a link between the occurrence of sudden stratospheric warming (SSW) and tropospheric blocking events. However, the rarity of SSWs and the ubiquity of blocking events gave rise to controversies in the literature on the statistically significant and physically meaningful connection between both phenomena. The relationship between Northern Hemisphere tropospheric blocking and SSW events is examined in a multi-century climate simulation. This study provides for the first time a robust climatology of SSW-related blocking, being limited however by the ability of the model to simulate the real climate system. Nevertheless, some results presented here are supported by other studies exploring the stratosphere-troposphere relationships in reanalysis datasets or for individual case studies. Overall, the results show a robust connection between the occurrence of SSWs and blocking in both the Euro-Atlantic and Pacific regions. The 40-day periods preceding and following the onset date of SSWs are marked by an enhanced frequency of blocking days in the Euro-Atlantic region and a reduced frequency in the west Pacific, with a significant shift in the distribution of blocking lifetime toward longer Eurasian blocks before the warmings and shorter west Pacific blocks after the onset of SSWs. During the weakening and breakdown of the stratospheric polar vortex, blocking events initiate, grow and displace in connection with large-scale disturbances of planetary waves 1 and 2. Finally, the results further indicate that once the SSWs initiate, an enhanced frequency of short-lasting blocking events at the expense of long-lasting blocks is associated with a rapid weakening of large-scale planetary wave anomalies and an increased wave contribution from smaller-scale disturbances.

Keywords Stratosphere-troposphere interaction · atmospheric blocking · sudden stratospheric warming · multi-century climate simulation · Northern Nemisphere

Jessica Vial
Climatic Research Unit, School of Environmental Sciences, University of East Anglia, Norwich NR4 7TJ, United Kingdom
E-mail: j.vial@uea.ac.uk

Tim J. Osborn
Climatic Research Unit, School of Environmental Sciences, University of East Anglia, Norwich NR4 7TJ, United Kingdom

1 Introduction

1.1 What is a sudden stratospheric warming?

SSWs are considered to be the most dramatic large-scale phenomena to occur in the extratropical stratosphere during the winter/spring seasons (Andrews et al, 1987). Such events are characterised by temperature rises and weakening of the zonal-mean zonal flow in the stratosphere, which lead to major disruptions of the large-scale and persistent polar cyclone (polar vortex). Two types of warming events have been identified: the *vortex displacement* event when high potential vorticity over the pole is displaced equatorwards and takes the form of "a comma shape", and the *vortex splitting* event when the polar vortex splits into two distinct pieces (Charlton and Polvani, 2007).

Dynamical perspective

A dynamical model of the SSW, pioneered by Matsuno (1971) and now widely referred to in the literature, is based on the idea that SSW is initiated via the interaction between the stratospheric polar zonal flow and amplified vertically propagating planetary waves (PWs), consisting primarily of zonal wavenumbers 1 and 2. Such amplification of the PWs is due to tropospheric disturbances, which can manifest as blocking events (Andrews et al, 1987), or through the non-linear evolution of baroclinic eddies (Scinocca and Haines, 1998) or due to forcing at the surface (e.g., anomalous land/sea thermal contrasts, variation in snow cover). The stratosphere has to be in a specific state if a warming has to follow, such that PWs can propagate focusing toward the polar vortex instead of following their equatorward climatological path. The polar vortex is usually preconditioned when the zonal flow is displaced poleward and gets constricted about the pole (Andrews et al, 1987; McIntyre, 1982).

Upward propagating PWs are associated with poleward heat transport. Divergence equatorward and convergence poleward of the maximum eddy heat flux result in a weakening of the equator-to-pole temperature gradient, and according to the thermal wind balance, the vertical wind shear must weaken as well. From the continuity of mass, this is achieved by poleward motion at low levels, turning eastward because of the Coriolis effect, and equatorward at high levels with a westward Coriolis deviation. As a result there is (1) an easterly acceleration in the high atmosphere, (2) an upper-atmospheric adiabatic warming due to the rising motion associated with the "wave-induced meridional circulation", and causing the warming of the polar stratosphere.

1.2 Relationships between stratospheric sudden warming and tropospheric blocking: a review

It is widely believed that there is a connection between SSW and blocking events; several cases studies have been described and longer datasets have been analysed for that purpose, but the literature doesn't yet provide strong and clear evidence of a statistical or dynamical link between both phenomena. Labitzke (1965) investigated, by means of daily synoptic maps, the Northern Hemisphere tropospheric conditions before and after 11 pronounced stratospheric warming events that occurred in the winter seasons between 1957/58 and 1963/64. The SSW events were then divided into two categories with respect to their origin and direction of movement, namely the European and American SSWs. It was found that about 10 days after the onset of all of the European SSWs, blocking patterns formed and persisted from 1 to 3 weeks. However, those results are not entirely suported by the statistical study of Quiroz (1986), in the sense that blocking events led 17 of the 20 stratospheric warming episodes (85%) considered, by an average of 3.5 days, in contrast to the 10-day lag found in Labitzke (1965). Another example is the severe winter conditions experienced in the United States in 1936 and 1977, which are believed to be the results of large-scale blocking highs, during which a SSW and blocking events were simultaneously observed and preceded by amplifying stationary waves (Tung and Lindzen, 1979). Later, Naujokat et al (2002) argued that the occurrence of free traveling Rossby waves interacting with orographically and/or thermally forced stationary waves of zonal wavenumber 1 have led to three major warming events in December 1987, 1988 and 2001. In addition, they claimed that strong blocking episodes over the north Atlantic could have triggered these travelling waves before the warming initiated. This possible relationship was based on the fact that periods of blocking occurrence were almost coincident with the periods of travelling waves. So, whether the blocking caused the anomalous wave avtivity or vice versa does not seem to be so clear (Baldwin and Dunkerton, 1989).

More recently, Taguchi (2008) performed a statistical analysis, using a random bootstrap method, with 49 years of NCEP-NCAR reanalysis data from 1957/58 to 2005/2006, and considered two hypotheses that blocking events occur preferentially and last longer (1) in a pre-SSW period (blocking leads SSW by 10 days) or (2) in a post-SSW period (blocking follows SSW within a 60-day window). In contrast with previous studies, no significant association between SSW and blocking events were found. Contradictory results were then reported by Martius et al (2009), who did find a significant link between SSW and blocking events: 25 of the 27 SSW events analysed in ERA-40 for the period 1957-2001 were preceded by blocking patterns within a time lag of 10 days. In addition, their study revealed a strong correlation between the type of stratospheric events and the geographical location of blocking. Vortex displacements were mostly associated with Atlantic blocks, while for vortex splitting events blocking in the Pacific or in both the Atlantic and Pacific simulteanously were observed. Woollings et al (2010) examined the relationship between stratospheric variability and tropospheric blocking for the 44 boreal winter seasons from the reanalysis ERA-40 and a well-resolved stratosphere GCM

from the Hadley center (HadGAM). An empirical orthogonal function (EOF)-based approach was used to capture the stratospheric variability, rather than just stratospheric sudden warming events, in order to ensure more robust blocking-SSW links. It was found that the occurrence of blocking in different regions of the Northern Hemisphere, namely Europe, Greenland and west Pacific, modified the long stationary and/or transient tropospheric PWs (consistent with Naujokat et al (2002)'s hypothesis), which led to upward propagation of these long wave anomalies into the stratosphere. Blocking influenced the stratosphere via PW activity, while the inverse influence, which appeared to show a stronger signal, was via the mean zonal flow and downward propagation of annular mode variations from the stratosphere to the troposphere.

Two main reasons could explain the difficulty in establishing a robust link between tropospheric blocking and stratospheric warming events. First, the rarity of SSWs (at most once a year, Andrews et al (1987)), and the relatively short time-period of observational or analysed datasets (the first observation of SSW was made in 1952, Andrews et al (1987)), result in small sample size of SSW catalogues for statistical analysis (between 25 and 40 SSWs can be identified in a typical 45-year reanalysis dataset depending on the definition used, see references above). The second reason is that tropospheric blocking occurs frequently at different locations within one year, so that at first glance most of SSWs appeared to be associated with blocking events (Taguchi, 2008), although it might not be statistically or physically meaningful. The related difficulty arising from ubiquitous blocking events is in establishing which blocking regions are linked with SSWs and at which time-lag (Woollings et al, 2010).

1.3 Aim and outline

In this study, the relationships between SSW and tropospheric blocking events is revisited with an attempt to alleviate these problems. A 1000-year model simulation is used to increase the sample size of the SSW catalogue and provide more robust dynamical interpretations of the statistical stratosphere-blocking relationships. The precursor role of blocking on SSWs and the influence of SSWs on blocking are explored over a much larger sample size than previously used and over the different regions affected by blocking. Implications regarding the dependence between the annual cycle of blocking activity and the breaking of the stratospheric polar vortex are also considered. As a context for this study, when the stratospheric conditions change from sudden warming to a more climatological state, is there a change in tropospheric blocking variability?

The paper is organized as follows: Sections 2 and 3 describe the model and methodology, respectively. Some results concerning the temporal evolution of tropospheric and stratospheric features closely related with blocking are presented in Section 4. The relationship between the occurrence of SSWs and blocking episodes is analysed in more details in Section 5. Finally, Section 6 contains a summary of the main results.

2 Model simulation

The simulation used in this study is the 1000-year (nominally 1800-2799) Pre-industrial Control experiment of the LMDZ fifth-generation atmosphere-ocean coupled model, prepared for the Coupled Model Intercomparison Project Phase 5 (CMIP5). Its atmospheric component (LMDZ5) uses a horizontal resolution of 1.9° in latitude and 3.75° in longitude and 39 levels in the vertical (96x96L39)[1]. The Pre-industrial Control experiment (hereafter, PiControl) imposes non-evolving and pre-industrial prescribed atmospheric concentrations of all well-mixed gases (including CO_2), and emissions or concentrations of natural aerosols (Taylor et al, 2009). As there is no external forcing and no climate change signal, this experiment can be used to estimate the unforced internal variability of the coupled model, which mainly refers to the annual cycle and developing temporal and spatial scales variations due to different conditions within the period of integration. This simulation is therefore very useful to understand the climate dynamics in the model.

3 Methodology

3.1 Detection of stratospheric sudden warmings

The methodology for the detection of SSW events is adaptated from Limpasuvan et al (2004). The variability in the strength of the polar vortex is determined from the leading principal component (PC) associated with the first empirical orthogonal function (EOF) of the zonal-mean zonal wind

[1] Model documentation and further reference are available at http://icmc.ipsl.fr

anomalies[2] at 10 hPa.
When performing an EOF analysis, the data in the spatial domain have to be area weighted prior to calculation to account for the convergence of the meridians, which reduces the impact of high-latitude grid points. Here, the data are weighted by the square root of the cosine of latitude, as it is commonly used in the climate community (e.g. Limpasuvan et al (2004)). The only important characteristic of the EOFs is the spatial pattern of variance that they represent, the signs and units of the EOFs being totally arbitrary. As shown in Figure 1 (top), the leading EOF structure of the zonal-mean zonal wind anomalies at 10 hPa represents a dipole pattern with a reversal of sign at about 40°N. The sign and amplitude of the pattern as a function of time are then given by the PC associated with the corresponding EOF, and which is obtained by projecting the weighted data anomaly onto the leading EOF. The leading PC time series explains about 62% of the total variance in the 10 hPa zonal-mean zonal wind field, and negative values correspond to weaker than normal westerlies poleward of 40°N.
The same EOF analysis was performed in Limpasuvan et al (2004) at 10 hPa and 50 hPa, and it was found that the results were reasonably insensitive to the stratospheric level, although at 10 hPa the leading PC/EOF was not as clearly separated from the higher modes as was the case at 50 hPa.

The occurrence of a SSW event is determined from the amplitude of the PC time series, low-pass filtered with a 15-day boxcar average. The onset date of a SSW event is defined when the low-pass PC drops more than one standard deviation below its climatological mean ($-\sigma$), and the decay date is when the low-pass PC rises again above $-\sigma$. Here, $-\sigma \simeq 18.1\ m/s$. A SSW event (from onset to decay) must last at least 20 days, and two consecutive onset dates (within one year) must be separated by at least 120 days, to minimise the occurrence of overlapping periods preceding and following SSW events. Overall, 672 SSW events were detected based on the above criteria. The onset dates associated with these events occur between mid October and end of April, with a maximum frequency in January (Fig. 1, bottom). Similar results were found in Lott et al (2005) using a 20-year integration of the upward extended atmospheric-only LMDZ model. Only SSW events whose onset dates are between the 1^{st} of December to the 31^{st} of March are selected for this study, which reduces the number of SSW events to 480.

[2] All anomalies in this study are deviations from the daily climatological seasonal cycle calculated from the 1000-year simulation.

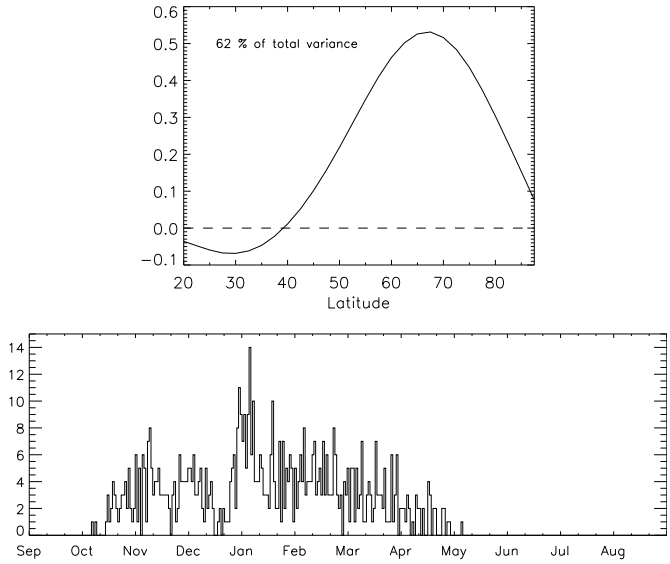

Fig. 1 Top: The leading EOF structure of the zonal-mean zonal wind anomalies at 10 hPa. Bottom: Occurrence of the 672 SSW onset dates from 1 January 1800 to 31 December 2799, computed from the amplitude of the low-pass filtered PC time series.

3.2 Detection of tropospheric blocking

The blocking index has been calculated, following the methodology described in Vial and Osborn (2011), at daily intervals during the extended winter (ONDJFMAM, October to May) season throughout the 1000 years of the PiControl simulation (1 October 1800 - 31 May 2799). The ONDJFMAM season is chosen because SSWs occurring in DJFM may be associated with tropospheric signals well before and after their onset dates. Here, the 2-month periods preceding and following the onset date of SSW events are inspected. The model output has been regridded (using bilinear interpolation) to 2.5° resolution, and the blocking index is calculated at each longitude and time step across the whole Northern Hemisphere. The central latitude of blocking is taken as the latitude of the maximum storm track intensity (corresponding to the mean storm track latitude calculated for the individual months from October to May). In order to account for the annual cycle in the position of the storm track latitude (not shown), the blocking index is calculated at all latitudes with ±7.5° of the storm track latitude. At each specific longitude and time step, a local and instantaneous blocking candidate is assigned to the central blocking latitude where the zonal wind revearsal (Eq. 1 in Vial and Osborn (2011)) is the greatest.
In order to account for the annual cycle in the amplitude atmospheric variability, the anomaly

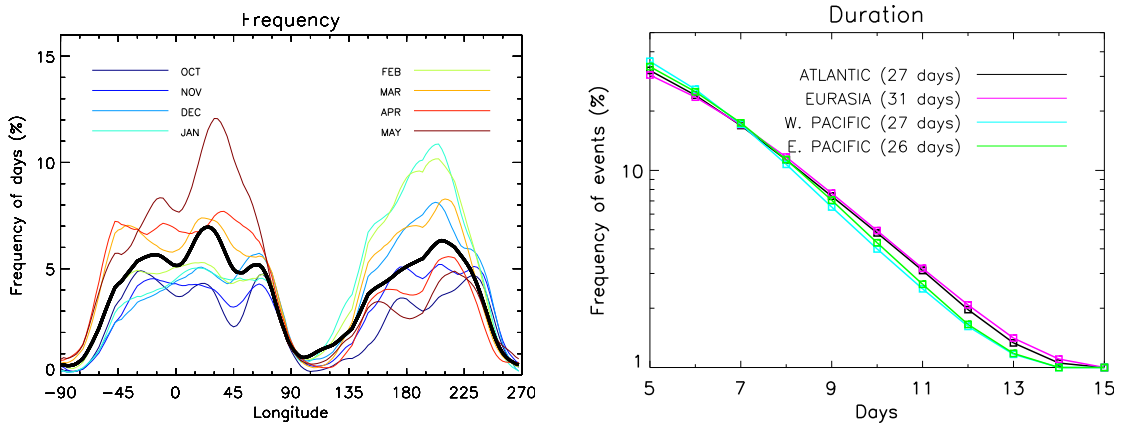

Fig. 2 (left) Frequency of all days that are part of large-scale blocking episodes as a function of longitude, for the ONDJFMAM period (thick black line). Monthly mean frequencies are displayed by the different colors, as explained in the legend. (right) The average frequency of large-scale blocking episodes (at least 5 days duration) as a function of their duration (days) for the Atlantic, Eurasian, western and eastern Pacific sectors. The maximum episode duration in each sector is indicated in brakets.

threshold at the location of the blocking anticyclone ($0.8 \times \sigma(Z')$ - Eq. 3 in Vial and Osborn (2011)) is allowed to vary with the month of the year by calculating the standard deviation (σ) from the 3-month daily anomaly distribution centered in the given month. Finally, a large-scale blocking episode is defined when a local and instantaneous blocking candidate spans at least 15° longitude and persists for at least 5 days.

For reference throughout this chapter, blocking frequency and duration have first been considered for the whole period of analysis during the ONDJFMAM season, and results are presented in Figure 2. The left panel illustrates the seasonal variability of Northern Hemisphere blocking frequency, with rising frequencies from a minimum in autumn to a sharp maximum in the late spring over the Euro-Atlantic sector. In the Pacific region, there is a tendency for more frequent blocks in winter and early spring (December to March) than in the temperate months. These results are in agreement with the works of Rex (1950) and D'Andrea et al (1998), but differ to some extent from those presented in Pelly and Hoskins (2003), who found for instance a maximum blocking frequency in autumn over the Euro-Atlantic sector. It must be noticed that different blocking indices, analysis periods, types of datasets (i.e., reanalysis or model simulation), contribute to the differences between the results presented here and those from previous works. However, widely recognized blocking features identified in the literature arise from the overall shape of the blocking distribution, presented in Figure 2 (e.g., geographical location, longer-lasting Euro-Atlantic than Pacific blocks). Note that a substantial amount of blocking episodes are also identified in the western Pacific region (between 135°E and 195°E). According to the results presented in Vial and Osborn (2011), an enhanced blocking activity in the western Pacific sector could be related to model systematic errors in the amplitude of the high-frequency variability.

The dependence between the seasonal variability of blocking activity and SSWs will be analysed in Section 5 on the basis of different blocking features between periods preceding and following warming events. The procedure to quantify the occurrence and persistence of blocking over different SSW-related periods will be described in Sections 5.1 and 5.2. In the remaining discussions throughout this chapter, periods preceding and following the onset date of SSW events are referred to as PRE-SSW and POST-SSW periods, respectively.

4 Temporal evolution of stratospheric sudden warming events

In this section, the temporal evolution of various atmospheric fields, composited for the 480 SSW events, is described. The fields analysed are the zonal-mean zonal wind anomalies (Fig. 3), and the large-scale planetary waves in geopotential height (Fig. 4). All fields are averaged between 45°N and 75°N, as it is the latitudinal band of interest for blocking and other midlatitude tropospheric disturbances that are potentially linked with stratospheric variability. Other stratospheric-based studies carried analyses within that range (Polvani and Waugh, 2004; Taguchi, 2008), at single latitude circles between 60°N and 85°N

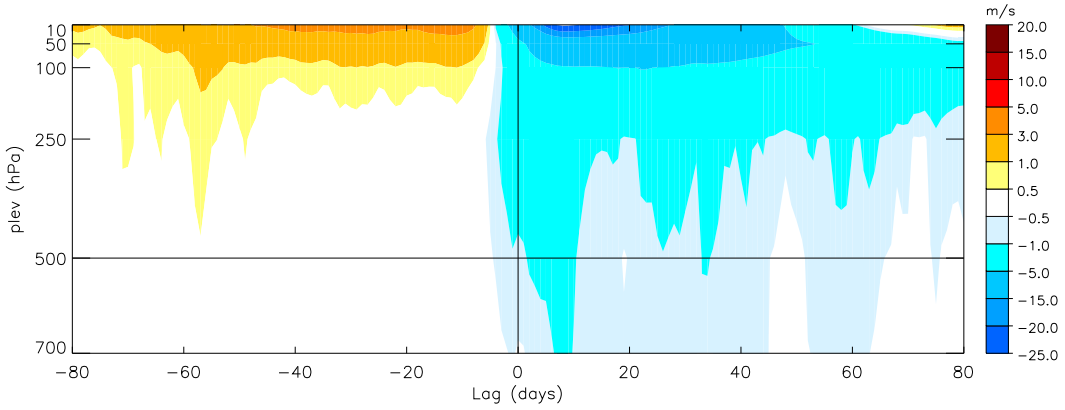

Fig. 3 Temporal evolution of the zonal-mean zonal wind anomalies as a function of height (in pressure level), averaged between 45°N and 75°N. The horizontal (time) axis is shifted with respect to the onset date of each of the 480 SSW events (lag = 0 days), and then the wind anomalies are averaged across all 480 events (aligned so that SSW onset is always at lag = 0 days).

(Limpasuvan et al, 2004) or at all latitude circles averaged above 50°N (Limpasuvan et al, 2004).

4.1 Zonal wind

The evolution of the anomalous zonal-mean zonal wind, composited for the 480 SSW events, is described. An average height profile of the zonal wind anomalies is calculated for each calendar day, spanning the 80-day PRE-SSW to the 80-day POST-SSW period, and is presented in Figure 3, where the time axis is shifted with respect to the onset dates of the SSWs. Due to the uneven temporal clustering of SSW events (Fig. 1, bottom), it is essential to remove the annual cycle of zonal wind before constructing this composite.

It exhibits a similar picture to that previously reported (Andrews et al, 1987; Limpasuvan et al, 2004), with a rapid weakening of the stratospheric zonal-mean zonal winds propagating down to the troposphere, where anomalous easterly winds then persist for up to two months. The rapid breakdown of the stratospheric zonal flow is preceded by anomalously strong westerlies, and is followed by the gradual recovery of the stratospheric polar vortex. In that sense, the SSWs are embedded in a low-frequency variability cycle, which assists in the preconditioning of the stratospheric zonal flow and the slow recovery of the polar vortex (Limpasuvan et al, 2004). The preconditioning of the polar vortex being initiated either by a precursor planetary wave (McIntyre, 1982), or as a result of the low-frequency stratospheric vascillation cycle, in which zonal flow anomalies oscillate meridionally and vertically on a time-scale of several months (Holton and Mass, 1976).

The time-scale at which anomalous easterly winds propagate between the 10 hPa and 500 hPa atmospheric levels is about 5 days, so that at lag = 0 days easterly anomalies have reached the 500-hPa tropospheric level (the level at which blocking events are identified in this study). Recall from Section 3.1 that the onset date is defined when the low-pass PC drops at least one standard deviation below its climatological mean, so lower amplitude anomalies at 10 hPa should be observed a few days before (when the low-pass PC drops below 0).

It is well established from previous studies that weak mid-tropospheric westerly winds provide favorable conditions for the formation of blocking events. For instance, Thompson and Wallace (2001) found more frequent blocking days over the Pacific and north Atlantic/Eurasian regions in the negative phase of the Northern Annular Mode (NAM), when high-latitude westerly winds are weaker than normal. Therefore it is reasonable to assume that the downward propagation of easterly wind anomalies seen in Figure 3 may have an impact on blocking activity. Following Thompson and Wallace (2001)'s results, blocking days are expected to be more frequent once SSW events initiate.

4.2 Planetary height waves

Next the evolution of the large-scale planetary height waves as a function of longitude and time at 10, 100 and 500 hPa is considered in Figure 4 to diagnose the existence of major wave disturbances throught the atmosphere that could possibly be linked with blocking.

Fourier Analysis

The Fourier analysis of the geopotential height field

$Z(\lambda, \phi, t)$ (hereafter, Z), performed in this study, is the decomposition of Z (averaged across the range of latitudes ϕ between 45°N and 75°N) into a sum of discrete harmonics (here, zonal wavenumbers), as:

$$Z = \overline{Z} + \sum_{n=1}^{N/2} Z_n cos\left(\frac{2\pi n}{N} - \lambda_n\right) \quad (1)$$

The overline represents the zonal mean at each time t, and each zonal wavenumber n is defined by its amplitude Z_n and phase λ_n at time t. The quantity $\frac{2\pi n}{N}$ is the angular frequency of the wave executing, n full cycles within the range (0, 2π) as the zonal index (longitude) varies from 0 to n (Wilks, 1995). Here, the original data is reconstructed by only retaining the individual wavenumbers $n = 1$ or $n = 2$ (denoted hereafter by PW 1 or PW 2, respectively), or the sum of $n = 1, 2, 3$ (denoted hereafter by PW 1..3). Note that PW 3 alone is not considered in order to show that its contribution in PW 1..3 is fairly minor compared to PW 1 and PW 2.

General structure of the wave composites

The wave composites in Figure 4 exhibit the same structure previously reported in three cases studies (Naujokat et al, 2002) and in the ERA-40 reanalysis dataset (Martius et al, 2009), with PW 1 tilting westward with height by nearly 180° between 10 hPa and 500 hPa, and PW 2 exhibiting a more barotropic structure with a phase shift of approximately 45°. In their composite analysis, Martius et al (2009) differentiated vortex displacement from vortex splitting SSW events, and they found that PW 2 tilts westward with height by approximately 90° for the displacement composite and 45° in the case of vortex splits. Another typical feature is the amplification of waves with height prior and during SSW events, which was found to be very strong for PWs 1 and 2 during splitting events, but nearly absent for PW 2 during displacement events (Martius et al, 2009). Similar results were reported in Charlton and Polvani (2007), showing that strong wave activity preceded splitting events but not displacement events. Further results showed that for vortex splits the amplitude of PW 2 is larger up to 100 hPa, while PW 1 exceeds it above that height (Martius et al, 2009). Figure 4 shows the same features observed during splitting events, with strong amplification for both PWs 1 and 2, PW 2 being larger below 100 hPa and lower above that level. It could therefore be assumed that the warming events considered in this study are mainly composed of vortex splits, with both PW 1 and 2 substantially contributing to the existence of these events. Of course, this assumption is only speculative, and it is beyond the scope of this study to differentiate displacement from splitting events.

Link between planetary scale waves and blocking

The importance of the geographical location of tropospheric blocking relative to planetary height waves was demonstrated in Martius et al (2009), and is used in this present study to infer a possible link between both phenomena at 500 hPa.

The strongest wave amplification (refer to PW 1..3 in Figure 4) in the Pacific region seems to be colocated with the climatological Aleutian low (between 120°E and 195°E, Vial and Osborn (2011)) and Pacific ridge (between 195°E and 255°E, Vial and Osborn (2011)) at that level. About 10 days before the warmings initiate, only PW 2 contributes to the amplification of the Pacific planetary ridge, where eastern Pacific blocks are usually observed. However, in the period following the warming, amplification of PW 1 seems to be the main contribution to the positive Pacific wave signal, PW 2 amplification being fairly short-lasting. Therefore, an increase in the occurrence of eastern Pacific blocks in association with PW 2 amplification a few days preceding the warming could be expected, while a more persistent impact in association with PW 1 would be observed in the period following the onset of SSWs.

Over the western Pacific sector, the contribution from PWs 1 and 2 is the same as over the east Pacific region, except that, with their inverted phase, they contribute to the strengthening of the Aleutian low (between 120°E and 195°E), and could therefore be associated with a decrease in the occurrence of western Pacific blocks.

In the Euro-Atlantic region (between 90°W and 90°E), the main signal in the global wave composite (PW 1..3) prior to the SSW onset date, seems to arise from the amplification of the planetary ridge over the Eurasian sector only (between 30°W and 90°E), with contributions from both PWs 1 and 2. However, once the warmings initiate PW 1 is the main source of wave disturbances over the Atlantic basin (between 90°W and 30°W), where (1) the amplitude of the negative height anomaly, presumably associated with the Icelandic low, decreases, and (2) the amplitude of the Eurasian planetary wave decreases as well. In the period preceding the warming, amplification of both PWs 1 and 2 over the Eurasian region may be associated with an enhanced occurrence of blocked days over that sector. Whereas in the period following the warming, the PW 1 contribution to decrease the amplitude of the negative height signal over the Atlantic region, and also, but at a lesser

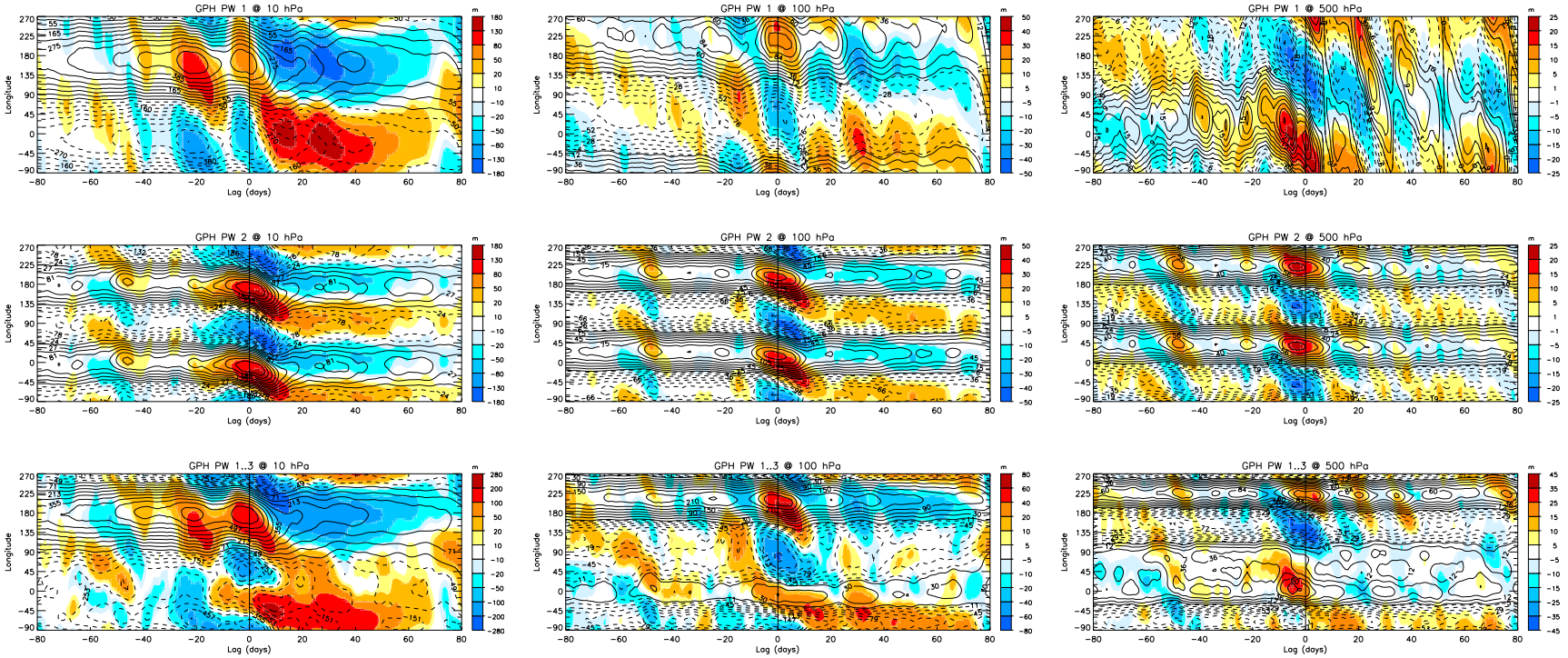

Fig. 4 Temporal evolution of the planetary height waves PW 1, PW 2 and PW 1..3, at 10, 100 and 500 hPa as a function of longitude, averaged between 45°N and 75°N. The horizontal (time) axis is shifted with respect the the onset dates of the 480 SSW events (lag = 0 days). Labeled black contours represent the full field; positive (negative) values are solid (dashed). Shaded areas are anomalies from the annual cycle. The structure displayed for PW 1..3 compared with the individual PW 1 and PW 2, suggests that the contribution of PW 3 is fairly small.

extent, the amplitude of the positive signal over the Eurasian sector, might provide more (less) favorable conditions for blocking development over the Atlantic (Eurasian) regions.

4.3 Hypotheses

Overall, this analysis identifies a plausible link between SSW events and blocking activity, according to which:

1. **In the period preceding the warming**, an amplification of PW 2 over the eastern Pacific region could be associated with an increased occurrence of blocking days over that sector, about 10 days prior to the warmings. However, it could be assumed that the Eurasian region would be the most affected, since a stronger amplification of the Eurasian planetary ridge takes place about 20 days prior the warmings, due to the contribution of both PWs 1 and 2. The western Pacific sector could, however, exhibit a reduced blocking frequency, with the contribution from both PWs 1 and 2.
2. **In the period following the warming**, the amplification and westward travelling of PW 1 is the main contribution to the global wave disturbances. This might be associated with an increased occurrence of blocking events in the Atlantic, and at a lesser extent in the eastern Pacific sector, whereas a slight decrease in blocking activity might be observed in the Eurasian and western Pacific regions. However, the downward propagation of the zonal wind anomalies could also contribute to perturb the blocking activity, increasing the occurrence of blocking days in either or all sectors.

5 SSW-related tropospheric blocking climatology

The aim of this section is to study the frequency and temporal persistence of atmospheric blocking throughout the Northern Hemisphere, and to look for evidence that these blocking characteristics vary depending on the period when they occur with respect to the onset date of SSW events.

5.1 Frequency of blocking days

Here the anomalous frequency of blocking days as a function of time and longitude, composited for the 480 SSW events, is described. For this to be done, an average longitudinal profile of the anomalous frequency of blocking days is calculated for each calendar day (i.e., with the annual cycle removed), spanning the 60-day PRE-SSW to the 60-day POST-SSW period, and is shifted with respect the the onset date of each of the SSWs (at lag = 0 days). A Hovmöller representation of anomalous blocking frequency spanning all longitudes can be seen in Figure 5.

The eastern parts of the north Atlantic (45°W-0°) and Eurasia (0°-90°E), as well as north Pacific (135°E-255°E) basins emerge clearly as regions where the anomalies in blocking frequency acquires their highest values (Fig. 5). As it was previously shown in Section 3.2, these regions are where blocking events are the most abundant on the climatological timescale (see also Figure 2).

An enhanced frequency of blocking days over the Euro-Atlantic sector is observed within the 40-day window period centered around the SSW onset dates (i.e., spanning approximately the 20-day PRE-SSW to the 20-day POST-SSW period). In general, the evolution of Euro-Atlantic blocks roughly coincides with periods of amplifying PW 1 and 2 (Fig. 4), which exhibit a slight wavenumber 1 amplification (up to 10 m) within the 40-to-10 day window preceding the warmings, and an abrupt and simultaneous increase (up to 25 m) in the amplitude of PWs 1 and 2 from 10 days before onset up to about 5 days after the onset date of the SSWs. Between lag_{+5} and lag_{+20}, PW 1 displaces over the Atlantic region, and PW 2 weakens, with a simultaneous longitudinal displacement of positive blocking frequency anomalies over the Atlantic basin, while the Eurasian region suffers a reduced frequency. The influence of PW amplification seems to persist beyond the 20-day POST-SSW period over the Atlantic region (although at a lesser extent), as positive anomalies in blocking frequency are observed up to lag_{+60}. These results support both hypotheses stated in Section 4.3, and provide further evidence that amplifying PWs may be associated with enhanced blocking activity over the Euro-Atlantic region before and after the onset of SSWs.

The tendency in the Pacific sector is a reduced frequency of blocking days over the western part of the region (135°E-195°E) spanning approximately the 15-day PRE-SSW to the 20-day POST-SSW period, and an enhanced frequency over eastern Pacific (195°E-255°E) within the 20-day window centered around the SSW onset dates. The evolution of blocking activity in this region coincides as well with periods of amplifying and decaying PW 1 and 2 (Fig. 4), with some resemblance to the structure of PW 2 amplification at about 45 days before onset, a strong

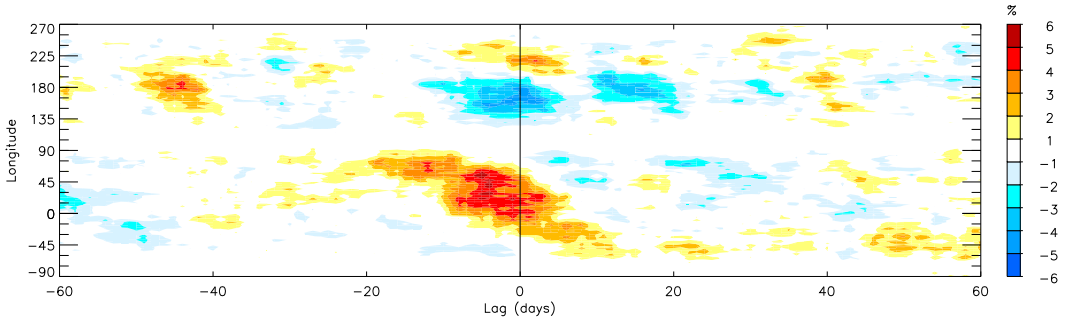

Fig. 5 Temporal evolution of the anomalous frequency of all days within the extended winter season (ONDJFMAM) that are part of large-scale blocking episodes (at least 5-day duration) as a function of longitude. The horizontal (time) axis is shifted with respect to the onset dates of the SSW events (lag = 0 days). The anomalous blocking frequency is the deviation from the daily climatological seasonal cycle, composited for all 480 SSW events. Note that anomalies in blocking frequency beyond lag_{-60} and lag_{+60} days cannot be displayed, since the detection of blocking events from October to May only allows a 2-month window on either side of the SSW onset dates (i.e., from lag_{-60} to lag_{+60} days).

decay in the amplitude of PW 1 between lag_{-20} and lag_{+20} over the whole Pacific region, and in PW 2 over the western part between lag_{-10} and lag_{+10}, while an amplification of PW 2 is observed over the east Pacific sector. As in the Euro-Atlantic region, these results support the existence of a link between blocking frequency and PW amplitudes over the Pacific region.

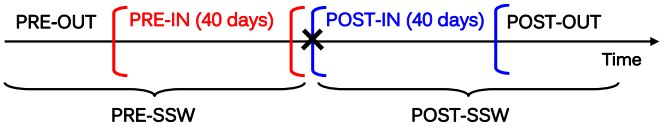

Fig. 6 Schematic representation of the four pre-defined periods in which blocking events are regarded to occur: PRE-IN (time lag = -40 to -1 days, in red), POST-IN (time lag = 0 to +39 days, in blue), PRE-OUT (all days before lag_{-40}) and POST-OUT (all days after lag_{+39}) periods, with respect to the onset date of SSW events (black cross).

5.2 Seasonal variability

A further analysis is now performed in order to analyse the influence of SSWs on the seasonal cycle of blocking activity, seen in Figure 2 (left panel). For that purpose, the frequency and persistence of blocking are computed in four different pre-defined periods (as illustrated in Figure 6) during SSW years only: PRE-IN and POST-IN (denoting the 40-day periods preceding and following, respectively, the onset date of SSW events), and PRE-OUT and POST-OUT (being all the remaining days before and after the PRE-IN and POST-IN periods, respectively). More generally, the periods containing all days that precede or follow the onset date of SSW events are referred to as PRE-SSW and POST-SSW, respectively. This analysis must ensures that relatively large periods are defined in order to not exclude long-lasting blocking episodes (i.e., 40 days was judged to be the minimum with respect to the climatological values - see Figure 2, right panel). Recall that 480 SSW events from 1 December to 31 March are selected for this study, so the number of days in each of the PRE-/POST-IN periods is $40 \times 480 = 19200$. The total number of days in PRE-/POST-OUT is 37462/40778.

SSWs are most frequent in January (Fig. 1) and the 40-day periods preceding and following the onset date of SSW events that are regarded as the PRE-IN and POST-IN periods, respectively, are more likely to be analysed in December, January and February (DJF). Therefore, PRE-OUT (POST-OUT) would correspond most often to October and November (March, April and May), and the differences in blocking features between those periods (if significant), would be representative of the influence of SSWs on the seasonal cycle of blocking activity.

In order to quantify the influence of the annual cycle on the results, a Monte Carlo test is performed, whereby blocking frequencies are computed within each of the four pre-defined periods, with respect to the same SSW onset dates, but using 480 years randomly selected from the 520 years without any SSW events. The same analysis is performed 100 times, from which a 95% confidence interval is constructed (for each of the four pre-defined periods). If SSWs have any relationship with blocking variability then the "real results" will lie outside the confidence interval of the 100 random results drawn from years without SSWs.

Results are presented in Figures 7 and 8, where the solid (dashed) lines are the blocking frequency (Fig. 7) and duration (Fig. 8) in the "real" SSW-related

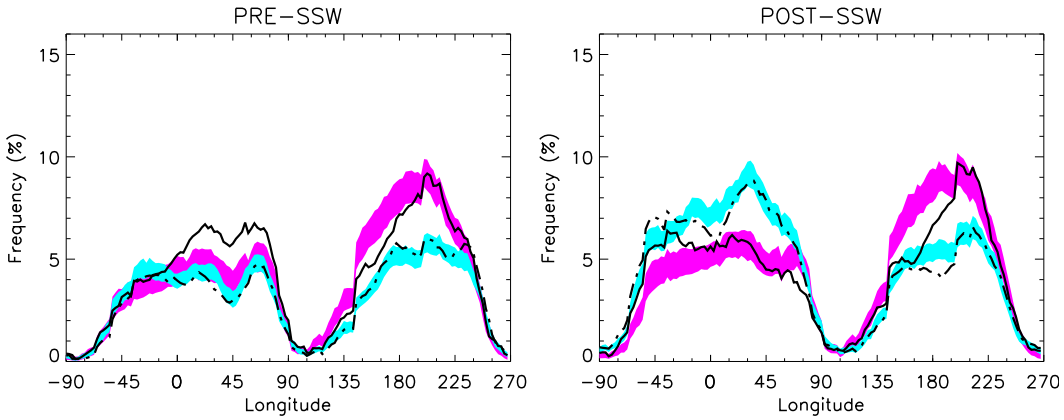

Fig. 7 Frequency of all days that are part of large-scale blocking episodes, as a function of longitude. Frequencies in the periods preceding the warmings (PRE-SSW) are displayed in the left panels, and frequencies following the warmings (POST-SSW) are displayed in the right panels. The solid (dashed) black lines represent the "real" PRE-/POST-IN (PRE-/POST-OUT) period and the magenta (cyan) are represent the 95% confidence interval of the PRE-/POST-IN (PRE-/POST-OUT) periods.

PRE-/POST-IN (PRE-/POST-OUT) periods. The magenta (cyan) areas are the 95% confidence interval for the "random" SSW-related PRE-/POST-IN (PRE-/POST-OUT) periods.

5.2.1 Blocking frequency

Results presented in Figure 7 are consistent with those of Figure 5, with an enhanced frequency of blocking days over the Eurasian (Atlantic) in PRE-IN (POST-IN), and a tendency for a reduced frequency of western Pacific blocks in those two periods (compare the solid lines and magenta areas in the PRE- and POST-SSW panels). Note that, although the changes in blocking frequency between the "real" and "random" cases seem to be small, they are significant at the 95% confidence level. In addition, it is worth recalling that these results are drawn from a 1000-year simulation, so they are smoothed by the diversity of the tropospheric responses to stratospheric disturbances, and therefore are even more robust than if they were drawn from a smaller sample size dataset. In the PRE-/POST-OUT periods, the frequency of blocking is not significantly affected by SSW events, as the "real" SSW-related blocking frequencies lie within the confidence intervals (compare the dashed lines and the cyan areas). In the POST-OUT period, there are occasional longitudes in the Atlantic and central Pacific sectors where the SSW-related frequency is slightly (but significantly) different from the "random" POST-OUT period, suggesting that the influence of SSWs tends to persist longer than 40 days, as it is observed in Figure 5 and reported in other studies (e.g., Thompson et al (2002)). Nevertheless, most of the significant SSW-related signal is within the PRE-/POST-IN periods (presumably spanning the 20-day PRE-SSW to the 20-day POST-SSW period according to Figure 5). Overall those results suggest that the seasonal cycle of blocking frequency is significantly related to stratospheric flow disturbances over the Euro-Atlantic and west Pacific regions, where wintertime blocking frequency is enhanced (reduced) in the former (latter) in years when SSW events occur. No significant relationship is found in autumn and spring.

5.2.2 Blocking duration

The frequency of large-scale blocking episodes as a function of their duration in the Atlantic, Eurasian and Pacific sectors are presented in Figure 8, during the "real" PRE-/POST-IN and PRE-/POST-OUT periods (solid and dashed lines, respectively), and "random" PRE-/POST-IN and PRE-/POST-OUT periods (magenta and cyan areas, respectively), obtained with the similar Monte Carlo approach as explained previously (i.e., using the timing of the SSW onset dates, but with data from random years without SSW events).

In the PRE-SSW period, the increase in the total frequency of blocking days over the Eurasian sector (Fig. 7, left panel), is associated with a significant shift in the distribution of blocking lifetime toward longer blocks (compare the solid line and magenta area in Figure 8, left panel, 2^{nd} row). This does not seem to be the case when the stratospheric signals propagate downward, increasing the frequency of blocking days in the POST-IN period over the Atlantic sector (Fig. 5 and 7, right panel), as the frequency of long-lasting blocking episodes (above 11-day duration) tends to decrease with respect to the POST-OUT period, although the results are not significant at the 95%

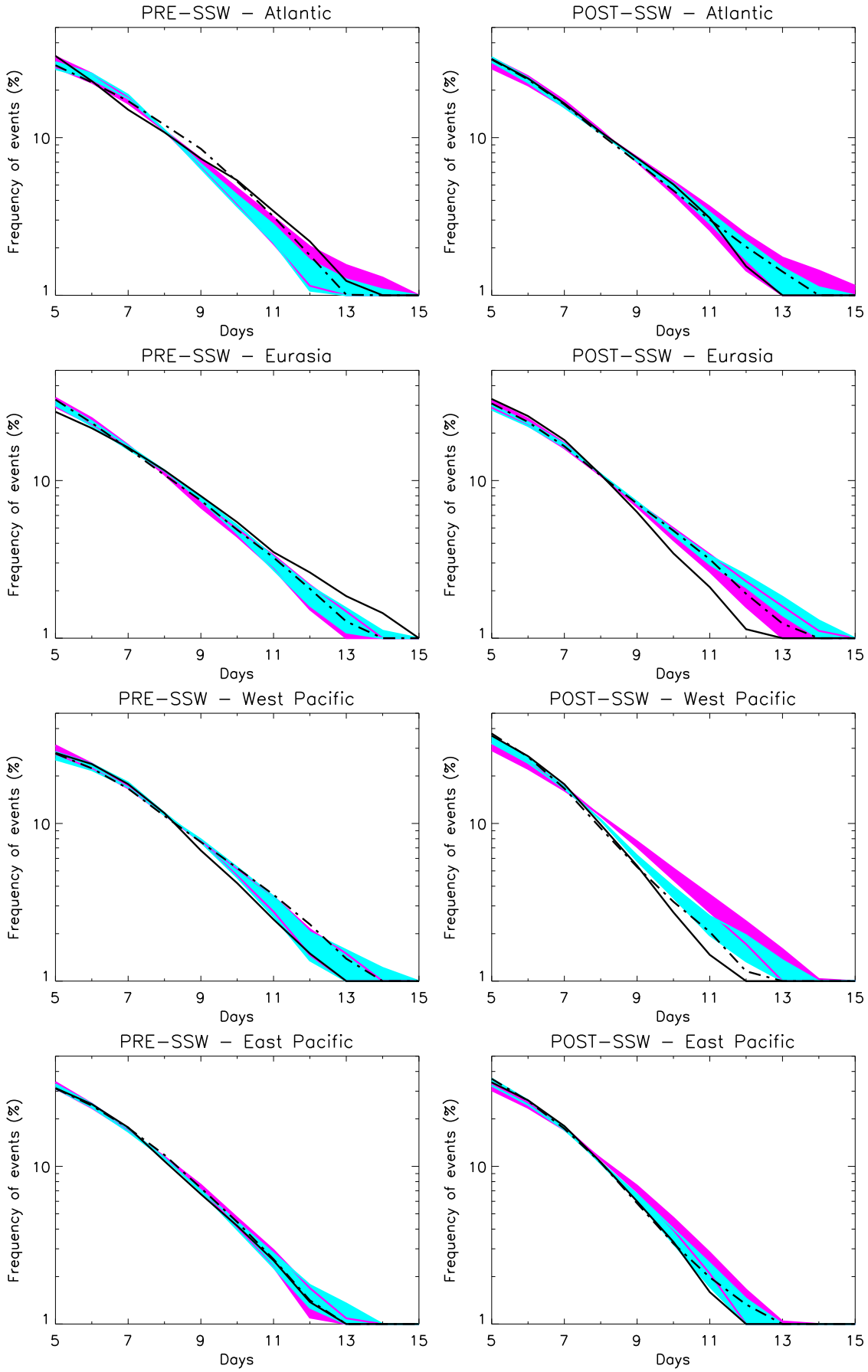

Fig. 8 Blocking duration defined as the average frequency of large-scale blocking episodes as a function of duration (in days) for the Atlantic (75°W-0°, 1^{st} row), the Eurasian (0°-45°E, 2^{nd} row), the west Pacific (135°E-195°E, 3^{rd} row) and the east Pacific (195°E-255°E, 4^{th} row) sectors. Frequencies in the periods preceding the warmings (PRE-SSW) are displayed in the left panels, and the periods following the warmings (POST-SSW) are displayed in the right panels. The solid (dashed) black lines represent the "real" PRE-/POST-IN (PRE-/POST-OUT) period and the magenta (cyan) are represent the 95% confidence interval of the PRE-/POST-IN (PRE-/POST-OUT) periods.

level (Fig. 8, right panel, 1^{st} row). In the west Pacific sector, blocking tend to be less frequent in POST-IN (and at a lesser extent in PRE-IN) than in POST-OUT (and PRE-OUT) (Fig.7), and this decrease seems to be related to a shift toward shorter blocks (with higher significance in the POST-SSW period in Figure 8, right panel, 3^{rd} row).
There are cases where the total frequency of blocked days is not significantly affected by the presence of SSW events, but the distribution of blocking lifetime is. In the Atlantic region, for instance, the frequency of PRE-OUT blocking episodes lasting between 7 and 13 days increases significantly (the dashed line lying outside the 95% confidence interval in Figure 8, left panel, 1^{st} row). Similarly over Eurasia, the distribution of POST-IN/OUT blocking episodes tends to be shifted toward shorter blocks (Fig. 8, right panel, 2^{nd} row), while no significant changes are found for the total frequency of blocking days (Fig. 7, right panel).
Overall it can be noticed that an increased (decreased) frequency of blocking days before the onset of SSWs seems to be associated with a shift in the distribution of blocking lifetime toward longer (shorter) blocks (i.e., for PRE-IN in Eurasia, west Pacific). However, when the frequency of days is not affected by SSWs, the frequency of long-lasting blocking episodes tend to be at the upper limit (or even above) the significance level (i.e., for PRE-IN/OUT in Atlantic, PRE-OUT in west Pacific - except in the eastern Pacific). This does not seem to be the case in the POST-SSW periods, as whether the frequency of blocking days is significantly affected by SSWs or not, there is a tendency for less frequent long-lasting blocking episodes in all regions (i.e., the frequencies of long-lasting blocking episodes lie at the lower limit or below the 95% confidence interval in Figure 8, right panels).

An attempt to explain this latter result is given by considering each contribution from large to smaller-scale waves within periods preceding and following the onset date of SSWs. For that purpose, the root mean squared (hereafter, RMS) PW anomalies, averaged over all longitudes, are computed for each latitude (between 0° and 90°N) and calendar day (spanning the 60-day PRE-SSW to the 60-day POST-SSW period). A Hovmöller representation of the RMS PW anomalies spanning all latitudes can be seen in Figure 9 for PW 1 (top), PW 2 (middle) and the sum of PWs 3 to 6 (bottom), along with their respective latitudinal average between 30°N and 75°N. By taking the RMS of PW anomalies, the amplitude only (not the phase) of PW anomalies (i.e., positive or negative anomalies) are being considered. In that way, the strength of the main wave disturbances related to the life cycle of SSWs are clearly quantifiable. The results in Figure 9 show that the first major change in wave amplitude for large- and small-scale disturbances is between 10 and 20 days before onset, with an average increase in the RMS PW anomalies of about 6-7 m for PW 1 and PW 2 and less than 2 m for PW 3+. Relatively high PW anomalies persist for about 30 days, up to lag = +15/+20 days. This period is then followed by a progressive weakening of PW 1 anomalies, while a more abrupt decrease is observed for PW 2 anomalies, so that between lag = +15 days and lag = +60 days the average strength of the large-scale PW anomalies returns to similar values as in the period preceding the amplitude increase at lag = -10 days. However, the amplitude of smaller-scale disturbances remains large (or even increases) after lag = +15-20 days (compared to the period preceding lag = -20 days). As a result, the contribution of small-scale disturbances to the global wave signal is higher in the POST-SSW (after lag = +15 days) than in the PRE-SSW (before lag = -15 days) period, as large-scale PW anomalies recover more rapidly to the breakdown of the stratospheric polar vortex.
It seems therefore plausible that in periods preceding the onset SSWs a larger contribution from large-scale than small-scale waves could enhance the frequency of long-lasting blocking episodes. However, in POST-SSW periods, a rapid weakening of large-scale planetary wave anomalies (i.e., PWs 1 and 2) and an increased wave contribution from smaller-scale disturbances (i.e., PW 3), could explain the enhanced frequency of short-lasting blocking episodes at the expense of long-lasting blocks.
Another interesting feature drawn from Figure 9 is a minimum in large-scale PW (i.e., PW 1 and PW 2) variance at 50°N-55°N after the onset of SSWs, being reminiscent of more contrasted (or more frequent) meridional dipole structures (e.g., high/low dipole blocks) in the POST-SSW than PRE-SSW period; the background flow seems to be more favorable to the formation and maintenance of dipole structures after the onset of SSW events.

The main conclusion drawn from this analysis is that, in the LMDZ climate model, the relationship between stratospheric flow disturbances and the seasonal cycle of blocking is different to some extent for the frequency and duration of blocking. Generally speaking, the occurrence of SSWs enhances (inhibits) the wintertime blocking frequency in the Euro-Atlantic (west Pacific) sector, while it has no influence in

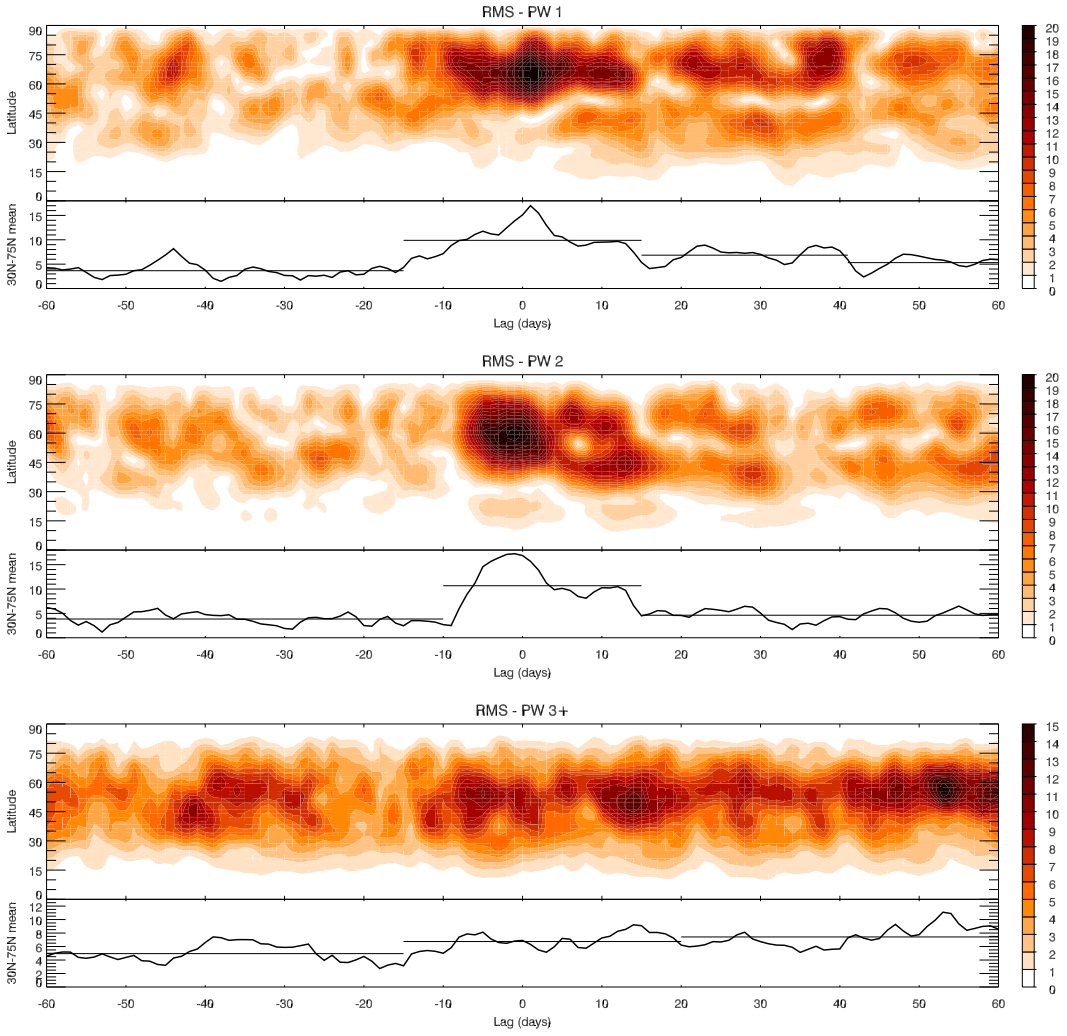

Fig. 9 Latitude-time Hovmöller representation of the root mean squared (RMS) PW anomalies averaged over all longitudes, computed for each for each calendar day, spanning the 60-day PRE-SSW to the 60-day POST-SSW period for PW 1 (top), PW 2 (middle) and the sum of PWs 3 to 6 (bottom). The horizontal (time) axis is shifted with respect the the onset dates of the 480 SSW events (lag = 0 days). The line plot in the lower part of each panel is the RMS PW anomalies averaged over all latitude between 30°N and 75°N; the horizontal lines represent time averaged periods. $RMS_l = \sqrt[2]{\frac{1}{N}\sum_{i=0}^{N}(pw_{i,l})^2}$, where $pw_{i,l}$ represents the PW anomaly at a longitude i and lag l from lag = -60 days to lag = +60 days; units are in meters (m).

autumn and spring. However, the proportion of long-lasting blocking episodes tend to be higher before SSW events than after, with in particular, a significant shift in the distribution of blocking lifetime toward longer wintertime Eurasian blocks in PRE-IN and shorter wintertime west Pacific blocks in POST-IN.

Synoptic description

Here the stratosphere-blocking link is examined in more details in order to synoptically describe how blocking may initiate, grow and displace in connection with planetary waves 1 and 2. For that purpose, 2-dimensional composite fields are constructed with respect to the onset date of SSW events (i.e., from lag_{-60} to lag_{+60} days). Figure 10 shows the 4-day average evolution of the 500 hPa daily height anomalies spanning the 60-day PRE-SSW to the 60-day POST-SSW period. This period is characterised by intense positive height anomalies over the Eurasian and east Pacific regions, roughly at the time and where blocking activity in those respective sectors is the strongest (Fig. 5). Therefore, the evolution of geopotential height anomalies will be taken as the base field to describe the evolution of those blocking events. In addition, anomalies in planetary waves 1 and 2, displayed in Figures 11 and 12 are used to qualitatively evaluate each contribution

in the stratosphere-blocking variability.

In the first panel (days -60:-57) of Figure 10, a middle latitude positive height anomaly located over the Eurasian sector moves westward and strengthens, accompanied by amplifying PW 1 and 2 also displacing westward, until they reach the east Pacific sector, with a strong anticyclonic anomaly at (days -44:-41). The following period (days -40:-17), the geopotential height flow is mostly characterised by small-scale anomalies, and small anomalous amplitudes in PW 1 and 2. At days -16:-13, another positive anomaly forms over the northern part of the Eurasian sector, and this time this anomalous anticyclone is accompanied by an amplifying PW 1 further toward the pole. At this time, there is also a weak negative height anomaly located over Canada, associated with a reinforcement of the negative wavenumber 1 signal at high latitudes. In the next panel (days -12:-9), the positive height anomaly strenghtens over the Eurasian sector, whereas the negative height anomaly moves south-westward, as it is pushed from southern latitudes by amplifying PWs 1 and 2. Within days -8:-5, a more prominent amplification of PWs 1 and 2 at high latitude is evident (Fig. 9, 11 and 12). Simultaneously, the anomalously high Eurasian anomaly substantially amplifies, where the positive wavenumber 1 and 2 signals increase, whereas the Pacific positive signal, mainly due to wavenumber 2, is associated with a developing anticyclonic anomaly over northwest Canada. From that period, the Pacific height anomaly increases and the PW 2 continuously amplifies, to both reach a maximum at days -4:3, and gradually decrease until the end of the period analysed. From the time when the Pacific anomaly is at a maximum, the anomaly decreases and also moves slowly westward over Alaska, with both PWs 1 and PW 2 being visibly associated with this displacement. The Eurasian height anomaly, although also dependent on the amplifying PW 2, seems to mainly evolve with PW 1, as they both increase until days 0:+3, when they start to slowly move westward over Scandinavia, and then more rapidly over the Atlantic basin, where they both decrease in amplitude. A strong anomalous geopotential height dipole over the Atlantic then persisted until days 36:39. After that period, the large-scale features of the flow slowly disapear, while smaller-scale disturbances start to re-appear. Note that the high geopotential height anomaly over Eurasia has been shown to be a precursor of weak stratospheric polar vortex events in other studies based on re-analysis or model simulation dataset (Kolstad and Charlton-Perez, 2011; Martius et al, 2009).

A few days prior the onset of the SSWs (days -4:-1) the strong anomalous anticyclonic anomalies in both the Pacific and Eurasian regions connect up via the polar region, and during the warmings anomalously high (low) geopotential heights are located over polar (mid-latitude) regions. As the vortex recovers, the positive height anomalies are then slowly displaced off the pole. During the warmings, simultaneous high-latitude blocking events in the Euro-Atlantic and Pacific regions are therefore expected. This is supported by the study of Woollings and Hoskins (2008), who found a significant link between the occurrence of high latitude blocking events in the Atlantic and Pacific sectors, with Atlantic blocking events leading Pacific blocks by 1-3 days. This quasi-simultaneous occurrence of blocks in the two sectors arise because of a large-scale distortion of the polar trough over Canada, initiated over southern Alaska and Greenland by developing anticyclonic anomalies, often in connection with a large-scale disturbance of the stratospheric polar vortex. The evolution of the simultaneous blocking events presented in Woollings and Hoskins (2008) is very similar to the synoptic description in this present study.

The retrogression of the anomalously high geopotential heights (blocking) seems to be linked with the low-frequency westward travelling large-scale planetary wave anomalies, favoring anomalously high blocking occurrence in various regions as they move. This is further supported by Naujokat et al (2002), who studied three individual blocking events in the north Atlantic, and suggested the possibility that blocking may initiate and decay on a timescale similar to that of the travelling wave period. Michelangeli and Vautard (1998) argued that one precursor of the Euro-Atlantic blocks is a high-latitude retrograding wavenumber 1 a few days preceding the blocking onsets. The anomalous westward-moving of PW 1 is also evident in the latitudinal average composite (Fig. 4), and is reminiscent of the Branstator-Kushnir 20-25 day oscillation (Branstator, 1987; Kushnir, 1987). Mid- or high-latitude tropospheric disturbances related to such oscillation cycles are characterised by westward motion and a life cycle of growth and decay over a period of about three weeks. The roughly concurrent occurrence of enhanced eatern Pacific blocks and anomalous westward-moving PW 1 (compare Figures 4 and 5) is also supported by Kushnir (1987) with the observation that large-scale

Pacific dipole blocking stuctures propagate westward and go through a life-cycle in phase with the 20-25 day oscillation.

This synoptic description provides further evidence that enhanced activity in both PW 1 and 2 are associated with an increased blocking activity at high latitudes over the Euro-Atlantic and northeast Pacific regions. The main changes in blocking activity (Fig. 5) and in the large-scale height field (Fig. 10) begin about 20 (10) days before SSW onset over the Euro-Atlantic (Pacific) region. Once the warmings initiate, amplitudes of PW 1 and 2 progressively decrease along with the anomalous anticyclonic conditions over the Pacific sector, while high geopotential height anomalies and stronger than normal blocking activity over the Euro-Atlantic region persist until the end of the period analysed.
The suggestion that the annual cycle of blocking activity over the Euro-Atlantic and Pacific basins could be strongly influenced by a low-frequency cycle of the stratospheric polar vortex, is supported by the synoptic evolution of anomalous height and PW fields being consistent with the blocking statistics seen in Figures 5 and 7. A large number of studies support the fact that some blocking events accompany amplifying PWs in the mid-troposphere (e.g., this is particularly well known for the amplification of the stationary waves, see Vial and Osborn (2011)), and that the preconditionning of the background flow could be more or less favorable for the development and maintenance of blocking (Martius et al, 2009; Naujokat et al, 2002).

6 Conclusion

The focus of this study has been to study the relationship between Northern Hemisphere tropospheric blocking and SSW events, in the long, multi-century IPSL-CM5A climate simulation. In particular, the precursor role of blocking on SSWs and the influence of SSWs on blocking were explored over the main regions affected by blocking (i.e., the Euro-Atlantic and Pacific sectors). The discussion advanced through the investigation of composites for a selection of fields, in an attempt to unfold aspects of the underlying large-scale dynamics that precede and follow the onset of SSWs in relation with the annual cycle of blocking activity. The use of a long climate model simulation provides a very much larger sample of SSW events than is available in the recent instrumental/re-analysis period, greatly increasing the power of the statistical analyses to distinguish real effects from random effects. This is limited by the ability of the model to simulate the real climate system, but this study also provides a valuable validation of the model, since some of the results presented here are supported by a number of studies exploring the stratosphere-troposphere relationships in reanalysis datasets or for individual case studies.
The main conclusion drawn from this analysis is that the entire low-frequency cycle during the weakening and breakdown of stratospheric polar vorter is associated with mid-tropospheric wave disturbances and anomalous circulations, which modulate to some extent the annual cycle in blocking activity. The occurrence of SSWs enhances the wintertime blocking frequency in the Euro-Atlantic region and inhibits it in the west Pacific sector, while no significant relationship was found beyond the 40-day periods preceding and following the onset date of SSWs (i.e., in autumn and spring, respectively). These SSW-related changes in blocking frequency were associated with a significant shift in the distribution of blocking lifetime toward longer wintertime Eurasian blocks in PRE-IN and shorter wintertime west Pacific blocks in POST-IN. Nevertheless, blocking episodes have a tendency to be more persistent before than after the onset date of SSWs. This latter results seems to be associated with a higher contribution of small-scale disturbances to the global wave signal in the POST-SSW than in the PRE-SSW.

Acknowledgements This work contributes toward a PhD funded by the School of Environmental Sciences at the University of East Anglia. The authors would like to acknowledge François Lott at the Laboratoire de Météorologie Dynamique, École Normale Supérieure (Paris), for his helpful comments and suggestions.

References

Andrews DG, Holton JR, Conway BL (1987) Middle atmosphere dynamics, vol 40. Academic Press

Baldwin MP, Dunkerton TJ (1989) The stratospheric major warming of early december 1987. Journal of the Atmospheric Sciences 46:2863–2884

Branstator G (1987) A striking example of the atmosphere's leading travelling pattern. Journal of the Atmospheric Sciences 44:2310–2321

Charlton AJ, Polvani LM (2007) A new look at stratospheric sudden warmings. part i: Climatology and modeling benchmarks. Journal of Climate 20:449–469

D'Andrea F, Tibaldi S, Blackburn M, Boer G, Déqué M, Dix M, Dugas B, Ferranti L, Iwasaki T, Kitoh A, Pope V, Randall D, Roeckner E, Straus D, Stern W, Den Dool HV, Williamson D (1998) Northern hemi-

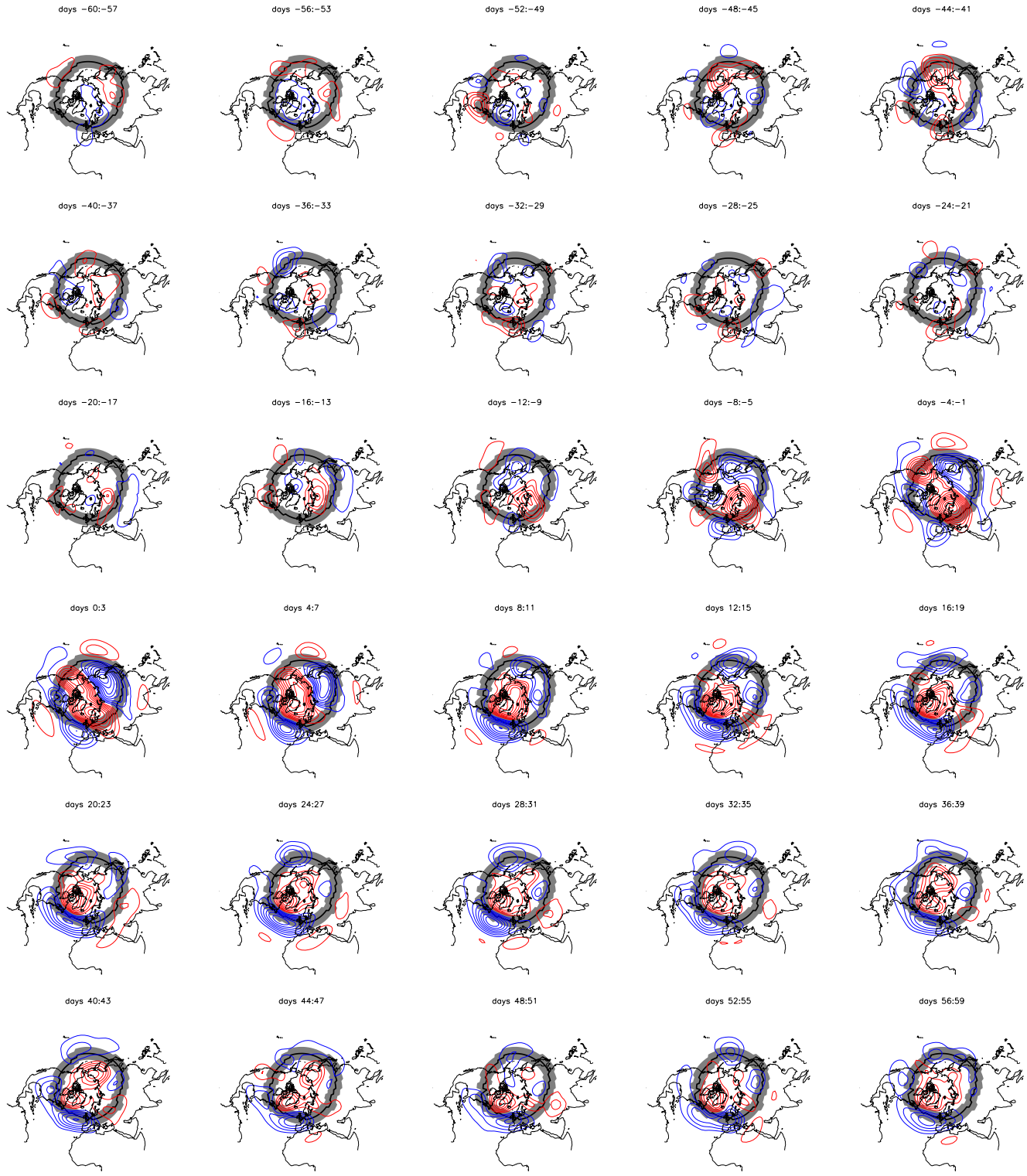

Fig. 10 4-day averaged daily geopotential height anomalies at 500 hPa spanning the 60-day PRE-SSW to the 60-day POST-SSW period. Positive height anomalies are displayed in red and negative anomalies in blue. Contours are drawn every 5 meters from -60 m to 60 m, but the zero contour is omitted. The solid black line is the central latitude of blocking, taken as the latitude of the maximum storm track intensity; the grey area represents ±7.5° around the storm track latitude allowed for blocking identification.

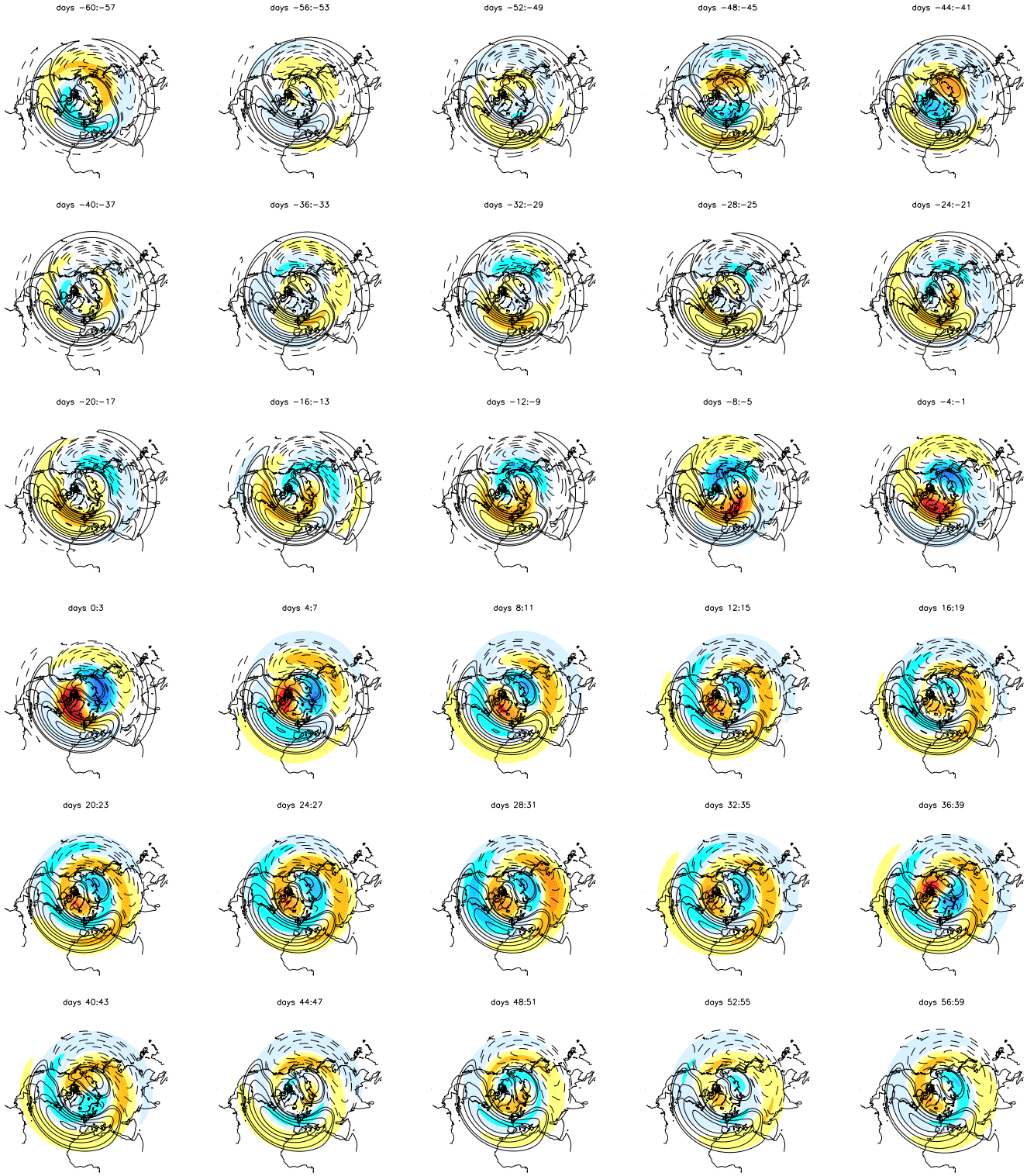

Fig. 11 4-day averaged planetary height wavenumber 1 at 500 hPa, for the same period and time intervals as in Figure 10. Contours are the full field given each 14 meters between -130 m and 130 m. Positive (negative) values are given as the solid (dashed) lines. Shaded areas are anomalies from the annual cycle with contour intervals at [-30,-20,-15,-10,-5,-1,1,5,10,15,20,30] meters.

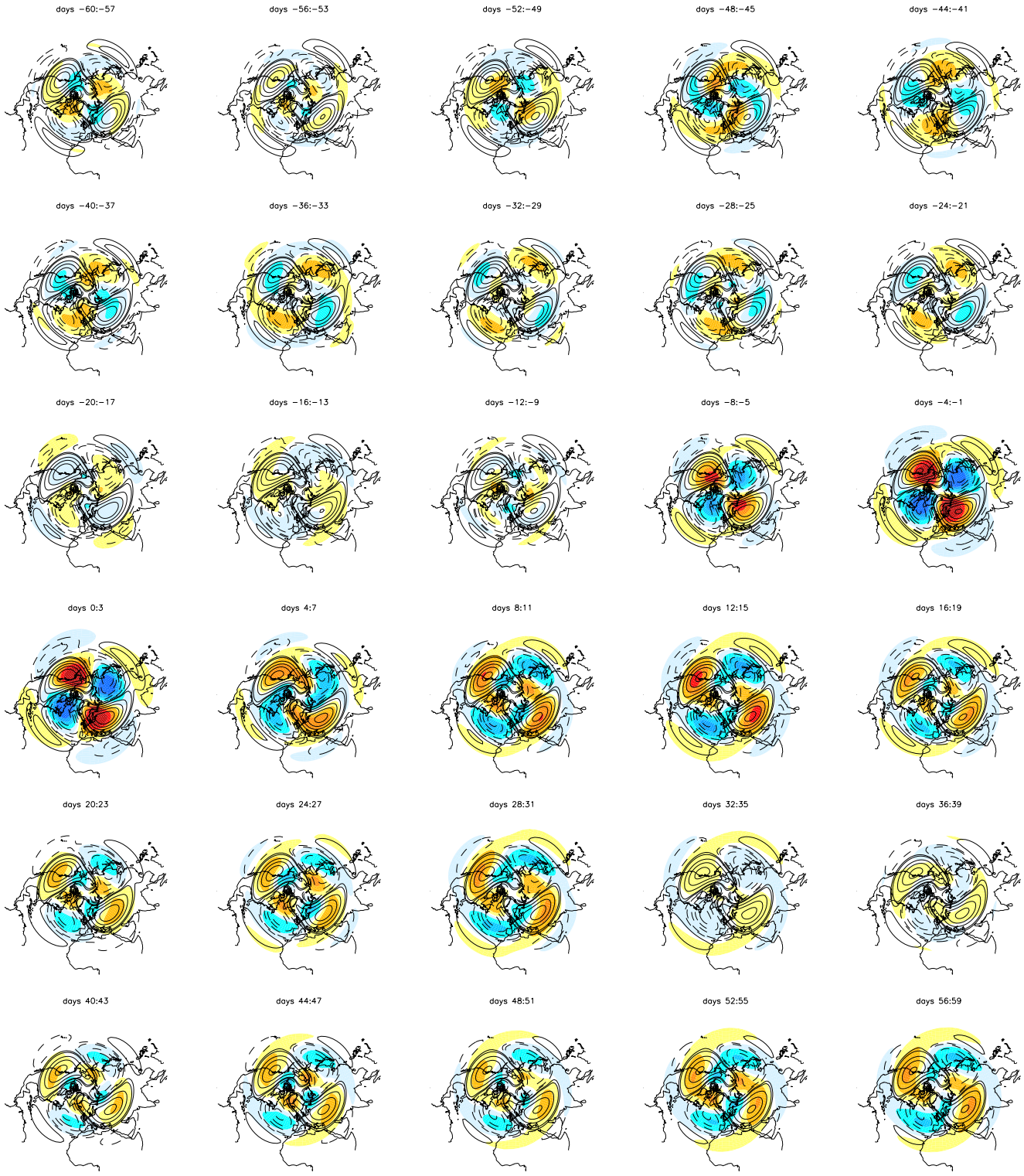

Fig. 12 Same as Figure 11 but for wavenumber 2. Anomaly contours are the same; full field contours are given every 12 meters between -110 m and 110 m.

sphere atmospheric blocking as simulated by 15 atmospheric general circulation models in the period 1979-1988. Climate Dynamics 4:385–407

Holton JR, Mass C (1976) Statospheric vascillation cycles. Journal of the Atmospheric Sciences 33:2218–2225

Kolstad E, Charlton-Perez A (2011) Observed and simulated precursors of stratospheric polar vortex anomalies in the northern hemisphere. Climate Dynamics 37:1443–1456

Kushnir Y (1987) Retrograding wintertime low-frequency disturbances over the north pacific ocean. Journal of the Atmospheric Sciences 44:2727–2741

Labitzke K (1965) On the mutual relation between stratosphere and troposphere during periods of stratospheric warmings in winter. Journal of Applied Meteorology 4:91–99

Limpasuvan V, Thompson DWJ, Hartmann DL (2004) The life cycle of the northern hemisphere sudden stratospheric warmings. Journal of Climate 17

Lott F, Fairhead L, Hourdin F, Levan P (2005) The stratospheric version of lmdz: dynamical climatologies, arctic oscillation, and impact on the surface climate. Climate Dynamics

Martius O, Polvani ML, Davies HC (2009) Blocking precursors to stratospheric sudden warming events. Geophysical Research Letters 36

Matsuno T (1971) A dynamical model of the stratospheric sudden warming. Journal of the Atmospheric Sciences 28:1479–1494

McIntyre M (1982) How well do we understand the dynamics of stratospheric warmings? Journal of the Meteorological Society of Japan 60:37–64

Michelangeli PA, Vautard R (1998) The dynamics of euro-atlantic blocking onsets. Quarterly Journal of the Royal Meteorological Society 124:1045–1070

Naujokat B, Kruger K, Matthes K, Hoffmann J, Kunze M, Labitzke K (2002) The early major warming in december 2001 - exceptional? Geophysical Research Letters 29(21)

Pelly J, Hoskins BJ (2003) A new perspective on blocking. Journal of Atmospheric Sciences 60:743–755

Polvani LM, Waugh DW (2004) Upward wave activity flux as a precursor to extreme stratospheric events and subsequent anomalous surface weather regimes. Journal of Climate 17:3514–3554

Quiroz RS (1986) The association of stratospheric warmings with tropospheric blocking. Journal of Geophysical Research 91:5277–5285

Rex D (1950) Blocking action in the middle troposphere and its effect upon regional climate. Part 2: the climatology of blocking action. Tellus 2:275–301

Scinocca JF, Haines K (1998) Dynamical forcing of stratospheric planetary waves by tropospheric baroclinic eddies. Journal of the Atmospheric Sciences 55:2361–2392

Taguchi M (2008) Is there a statistical connection between stratospheric sudden warming and tropospheric blocking events? Journal of the Atmospheric Sciences 65:1442–1454

Taylor KE, Stouffer RJ, Meehl GA (2009) A summary of the cmip5 experiment design

Thompson DWJ, Wallace JM (2001) Regional climate impacts of the northern hemisphere annular mode. Science 293:85–89

Thompson DWJ, Baldwin MP, Wallace JM (2002) Stratospheric connection to northern hemisphere wintertime weather: implications for prediction. Journal of Climate 15:1421–1428

Tung KK, Lindzen RS (1979) A theory of stationary long waves. Part I: A simple theory of blocking. Monthly Weather Review 107:714–734

Vial J, Osborn T (2011) Assessment of atmosphere-ocean general circulation model simulations of winter northern hemisphere atmospheric blocking. Climate Dynamics

Wilks DS (1995) Statistical methods in the atmospheric sciences. Academic Press

Woollings TJ, Hoskins BJ (2008) Simultaneous atlantic-pacific blocking and the northern annular mode. Quarterly Journal of the Royal Meteorological Society 134:1635–1646

Woollings TJ, Charlton-Perez A, Ineson S, Marshall AG, Masato G (2010) Associations between stratospheric variability and tropospheric blocking. Journal of Geophysical Research 115